QUARTERLY OF APPLIED MATHEMATICS
JANUARY, 1977

INTERACTION OF TWO VORTICES IN A FLUID WITH LOWER STAGNATION PRESSURE*

By

LU TING

Courant Institute of Mathematical Sciences, New York University

Abstract. The flow field induced by two point vortices of strength Γ at a distance $2h$ apart in a quiescent field with lower stagnation pressure is investigated. The flow field around the vortices is bounded by a free streamline with constant velocity U determined by the difference in the stagnation pressures. For the parameter $\Lambda = 2\pi hU/\Gamma > 1$, the flow field around each vortex is isolated from the other and is bounded by a circular free streamline of radius $\Gamma/(2\pi U)$. When $\Lambda = 1$, the two circular free streamlines just touch each other. When $\Lambda < 1$ the two flows merge and they are enclosed inside a single convex free streamline. Analytical solutions are presented for the merged flow field and the free streamline for the entire range of the parameter Λ.

1. Introduction. The stream function of a two-dimensional incompressible inviscid flow field induced by a point vortex in a quiescent fluid with lower stagnation pressure is

$$\Psi = \frac{\Gamma}{2\pi} \log r, \qquad r < R = \Gamma/(2\pi U).$$

Here r is the distance to the point vortex and U is the velocity along the circular free streamline of radius R outside of which is the quiescent fluid. The discontinuity in velocity across the free streamline accounts for the difference in the stagnation pressures of the fluids inside and outside the free streamline.

When there are two point vortices at a distance $2h$ apart with $h > R$, the parameter $\Lambda = 2\pi Uh/\Gamma$ is greater than 1. The flow field induced by each vortex will remain the same as that of a single vortex. When $\Lambda < 1$, the flows around the two vortices merge into a domain D in the x-y plane bounded by a closed free streamline ∂D (see Figs. 1, 2). The solution for the merged flow field and its boundary is presented in this paper. The stream function ψ satisfies the Laplace equation in D, i.e.

$$\Delta\Psi = 0, \tag{1}$$

with singularities representing the two point vortices in D. The boundary conditions on the free streamline ∂D are

$$\Psi = \text{constant}, \tag{2}$$

$$\partial\Psi/\partial\eta = U. \tag{3}$$

* Received June 4, 1975, The author wishes to thank Professor Joseph B. Keller for proposing this problem and for discussions. This research is supported by Grant AFOSR-73-2497A.

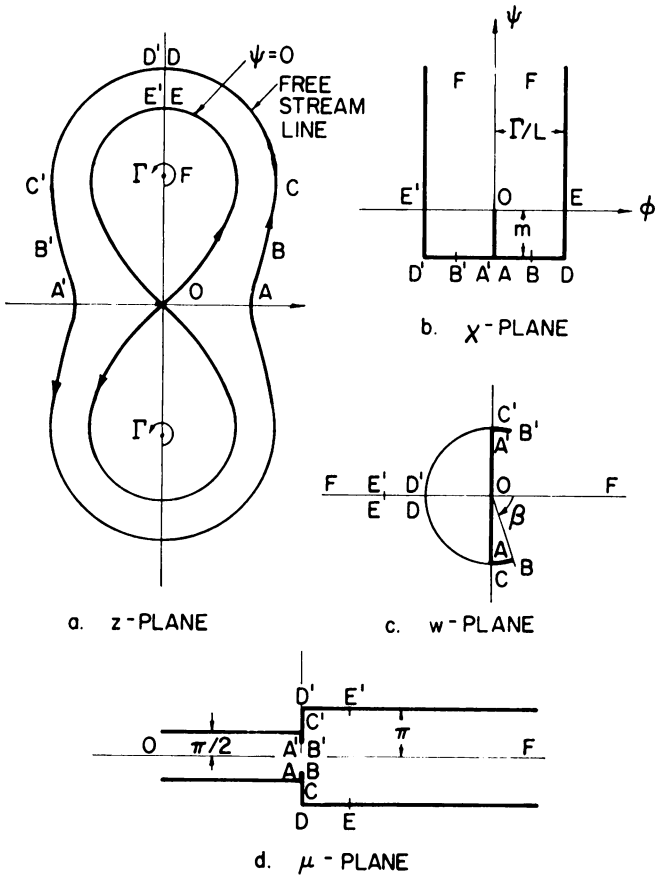

FIG. 1. The flow field with a necking of the free streamline at the middle section.

The solution will be constructed by the procedures for free streamline problems (see for example, [2]). The images of the flow field in the complex potential plane and in the hodograph plane are identified in Sec. 2 and the mapping functions and the final solution are presented in Sec. 3.

The result of this analysis can be applied to the simple models for the following problems:

i. Consider a two-dimensional turbulent free jet. The eddies in the jet are often simulated by vortices. When an eddy is transported to the outer edeg of the jet, where the stagnation pressure of the mean flow is much lower, the eddy will be stimulated by a circular vortex submerged in a stream of lower stagnation pressure. When two eddies come close together, the present solution will simulate when and how they merge into a single eddy.

ii. Consider a free jet with a large swirl. At each cross-section the flow field can be simulated by a vortical flow in a circle of radius R submerged in a fluid of lower stagnation pressure. When there are two free jets with large swirl and their axes intersect at a small angle, the distance between the center of the jet, $2h$, decreases gradually downstream and the two jets merge to a single one as h/R becomes less than 1. As the parameter h/R decreases, the present solutions represent the swirling flow at stations moving downstream.

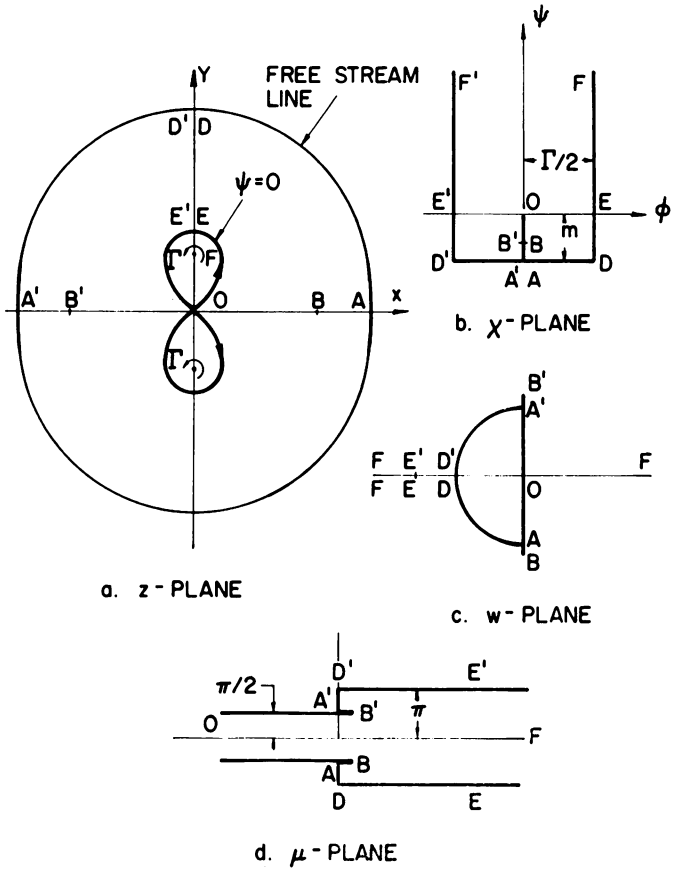

FIG. 2. The flow field with a convex free streamline.

The solution to this problem can also be interpreted as that for the lifting of a membrane glued under uniform tension to a flat surface, the x-y plane. Two concentrated forces are applied at a distance $2h$ apart to lift up the membrane. It will be assumed that the glue fails when the local linear normal force reaches the value N. If Ψ represents the height of the membrane above the domain D in the x-y plane where the membrane is separated from the flat surface, then we assume that Ψ obeys Eq. (1). The boundary conditions on ∂D are $\Psi = 0$ and $\partial\Psi/\partial\eta = N/T$. This problem is equivalent to the fluid-dynamic problem when the magnitude of the concentrated force is identified with ΓT and when N/T is identified with U.

2. The flow field and the hodograph plane. Fig. 1 shows two point vortices of equal strength Γ located in the complex z-plane, $z = x + iy$, at $z = \pm ih$ respectively. Due to the symmetry of Ψ with respect to y, it suffices to consider only the upper half plane, $y > 0$. The boundary condition on $y = 0$ is

$$\Psi_y = 0. \tag{4}$$

Also due to symmetry, $\Psi_x = 0$ on $x = 0$. Thus, the origin 0 is a stagnation point, i.e.,

$$\nabla\Psi = 0 \quad \text{at} \quad z = 0. \tag{5}$$

If Ψ represents the transverse displacement in the corresponding membrane problem, it is clear that along $y = 0$, Ψ is minimum with respect to y, Ψ vanishes at the two points A and A' on the free boundary and attains a maximum with respect to x at $x = 0$. At the origin, it is a saddle point.

In the complex velocity potential plane, the complex potential χ is set equal to zero at the stagnation point 0. Along the y-axis from the origin 0 to the point vortex F and along the x-axis from 0 to the point A on the free streamline, the potential φ is constant and is set equal to zero. Along the y-axis from the point F upward, a cut $DEFE'D'$ is introduced across which there is a jump of velocity potential from $\Gamma/2$ to $-\Gamma/2$ to account for the circulation around the vortex at F. In the χ-plane, point A is located at $-mi$ where m represents the unknown flux across the line $0A$. Along the free streamline ACD in the first quadrant $\Psi = -m$ and the potential increases from 0 at the point A to $\Gamma/2$ at the point D on the y-axis. The domain in the χ-plane representing the flow field in the first quadrant is the semi-infinite strip, $0 < \varphi < \Gamma/2$ and $-m < \Psi < \infty$. Its reflection with respect to the Ψ-axis represents the flow field in the second quadrant of the z-plane. In the χ-plane the vortex point F becomes $\Psi = \infty$ and $-\Gamma/2 < \varphi < \Gamma/2$.

In order to construct the image of the flow field in the hodograph plane, some physical understanding of the flow field is necessary. Due to symmetry, the free streamline will intercept the x-axis at A and A' at right angles. The distance $|AA'|$ will be either the maximum or the local minimum horizontal distance across the free streamline.

It seems realistic to assume that there is a finite range of the parameter Λ such that $|AA'|$ is a local minimum horizontal distance while the maximum horizontal distance across the free streamline occurs along $y = y_c > 0$ from point C to C' (see Fig. 1). At point C (and C') the tangent is also normal to the x-axis; therefore, there must be a point of inflection at B on the free streamline between points A and C. The inclination at B is denoted by β with $\pi/2 \geq \beta \geq 0$.

In the hodograph plane the complex conjugate velocity w is nondimensionalized by U, i.e.,

$$w = (|\nabla\Psi|/U) \exp(-i\theta) \tag{6}$$

where θ is the inclination of the flow with respect to the x-axis.

The image of the free streamline lies on the unit circle in the w-plane. The arcs BCD and AB of the free streamline are mapped into the arcs on the unit circle with $-\pi \leq \arg w \leq -\beta$ and with $-\pi/2 \leq \arg w \leq -\beta$ respectively. Points C and A have the same image, $w = -i$, in the w-plane. On the constant potential line $0A$, $\theta = \pi/2$; hence $0A$ is mapped into the downward radial line in the w-plane. It has been implied that the velocity along $0A$ increases monotonically from zero at 0 to U at A. The reflection of the w-plane with respect to the real axis represents the flow field in the second quadrant of the z-plane. The flow field above the x-axis is now mapped into the domain in the w-plane exterior to the left half of the unit circle, and to the two cuts ABC and $A'B'C'$ on the unit circle.

It will be shown in the next section that β and Λ can be related to a parameter d and that β is real only for $d \geq 2$. At $d = 2$,

$$\Lambda = \Lambda_c = [1 + (4/3) \log 2]/\sqrt{3} \sim 1.111, \tag{7}$$

$\beta = 90°$ and the cut ABC degenerates to one point. In this case, the center segment $|AA'|$ becomes the maximum horizontal distance across the free stream.

When d is less than 2, Λ is less than Λ_c ; the image of the flow field in the hodograph plane in Fig. 1 has to be changed. The center segment $|AA'|$ will now be the maximum horizontal distance across the free streamline and the inclination θ will increase monotonically along the free streamline from $\pi/2$ at A to π at D without a point of inflection (see Fig. 2a). On the other hand, the velocity along the potential line $0A$ will not be a monotonic function in x. This fact can be visualized by looking at the limiting case of $\Lambda \to 0$. Near the free streamline, the flow field should behave like that induced by a point vortex at origin with strength 2Γ and the velocity should increase inward from the free streamline. In particular, along the line AO, the velocity increases from U at A inward. On the other hand, point O is a stagnation point. Therefore, along the line AO the velocity increases from U at A to a maximum U_b at B and then decreases to zero at O, while the inclination θ remains $\pi/2$. The image of OA in the w-plane is along the downward radial line from the origin to point B outside the unit circle and then returns to point A on the unit circle. The free streamline AD is now mapped to the arc of the unit circle with $-\pi \leq \arg w \leq -\pi/2$. After the completion of the reflection with respect to the real axis, the image of the flow field in the w-plane becomes the domain exterior to the left half of the unit circle and the two cuts along the vertical radial segments AB and $A'B'$ (see Fig. 2c). It will be shown in the next section that this hodograph representation covers the range of Λ from Λ_c to zreo as d decreases from 2 to 1.

3. Conformal mappings and the solution. The flow field in the complex potential plane can be mapped into the upper half τ-plane by the Schwarz–Christoffel transformation [1]

$$\frac{d\chi}{d\tau} = \frac{ik\tau}{[(\tau^2 - 1)(\tau^2 - d^2)]^{1/2}}. \tag{8}$$

The image of points O, A, A', D, D' on the τ-plane are 0, 1. -1, d and $-d$ respectively with $d \geq 1$. It is easier to work in the ζ-plane with $\zeta = \tau^2$ (see Fig. 3). The mapping function is

$$\chi(\zeta) = \frac{ki}{2} \int_0^{\zeta} \frac{d\zeta}{[(\zeta - 1)(\zeta - d^2)]^{1/2}}. \tag{9}$$

The branch is picked so that the integrand is positive on the real axis with $\zeta > d^2$. The constants k and d are related to Γ and m since $\chi(d^2) - \chi(1) = \Gamma/2$ along the upper branch and $\chi(1) = -mi$. The results are

$$k = \Gamma/\pi, \tag{10}$$

$$m = (\Gamma/2\pi) \log [(d + 1)/(d - 1)]. \tag{11}$$

The flow field in the hodograph plane is mapped into the μ-plane with $\mu = \log w$ as shown in figures 1d and 2d. The mapping from the μ-plane to the upper half τ-plane is again accomplished by the Schwarz–Christoffel transformation:

$$\frac{d\mu}{d\tau} = \frac{J(\tau^2 - b^2)}{\tau[(\tau^2 - 1)(\tau^2 - d^2)]^{1/2}}. \tag{12}$$

Points B and B' lie on the real axis with $\tau = \pm b$ respectively. The mapping function

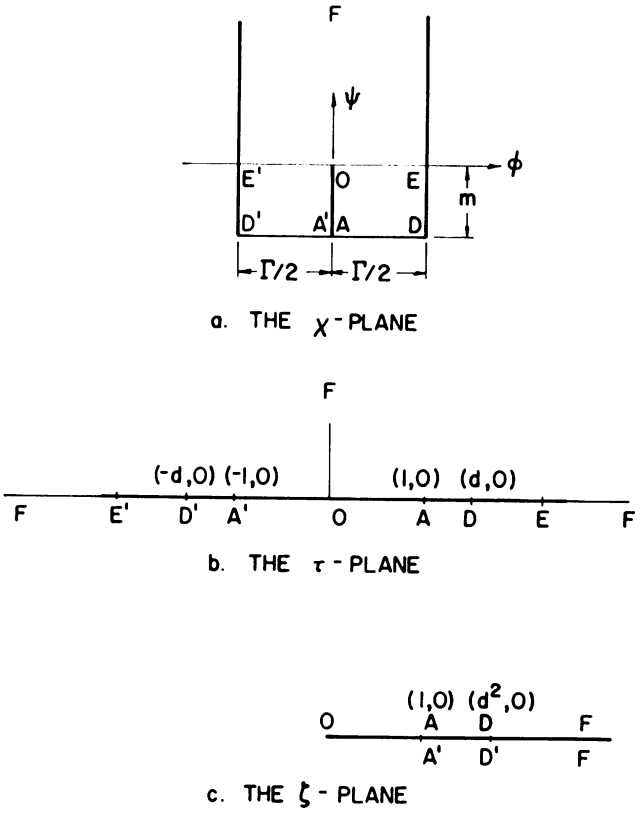

FIG. 3. Mapping of the χ-plane.

to the ζ-plane is

$$\mu + \frac{\pi}{2} i = \log w + \frac{\pi}{2} i = \frac{J}{2} \int_1^{\zeta} \frac{(\zeta - b^2)\, d\zeta}{\zeta[(\zeta - 1)(\zeta - d^2)]^{1/2}}. \tag{13}$$

Although the images of the flow field in the hodograph plane in Figs. 1 and 2 for the two different ranges of the parameter Λ are not the same, they have the same mapping function, Eq. (13). For the image of the w-plane in Fig. 1, the point B in the ζ-plane should lie between points A and D and hence $d \geq b \geq 1$. For that in Fig. 2 the point B in the ζ-plane should lie between O and A and hence $1 \geq b \geq 0$. This expectation of the ranges of b from physical reasoning will be confirmed later when the constant b is related to the parameter Λ.

Since the jump of μ from OA to OA' is πi, it should equal $J\pi i$ times the residue of the integrand in Eq. (13) at $\zeta = 0$. The result is

$$Jb^2/d = 1. \tag{14}$$

Another condition is that $\mu = -\pi i$ at D when $\zeta = d^2$ and Eq. (13) yields

$$J[1 - b^2/d] = 1. \tag{15}$$

These two equations become:

$$J = 2, \qquad b^2 = d/2. \tag{16}$$

The only unknown constant d will be defined by the condition that in the z-plane point F is located at hi. The z-plane is related to the ζ-plane by the relationship

$$dz = \frac{d\chi}{Uw} = \left(\frac{d\chi}{d\zeta}\right)\frac{d\zeta}{Uw}. \tag{17}$$

$w(\zeta)$ can be obtained by carrying out the integration of Eq. (13). This yields

$$\mu + \frac{\pi}{2}i = 2\log\frac{(\zeta - d^2)^{1/2} + (\zeta - 1)^{1/2}}{i(d^2 - 1)^{1/2}} - \log\frac{(\zeta - d^2)^{1/2} + d(\zeta - 1)^{1/2}}{i[\zeta(d^2 - 1)]^{1/2}} \tag{18}$$

and hence

$$\frac{1}{w} = \frac{-[(\zeta - d^2)^{1/2} + d(\zeta - 1)^{1/2}][(\zeta - d^2)^{1/2} - (\zeta - 1)^{1/2}]^2}{\zeta^{1/2}(d^2 - 1)^{3/2}}. \tag{19}$$

The relationship between z and ζ is

$$\left(\frac{2\pi U}{\Gamma}\right)z$$

$$= \frac{i}{(d^2 - 1)^{3/2}}\int_0^{\zeta}\frac{[(\zeta - d^2)^{1/2} + d(\zeta - 1)^{1/2}][2\zeta - d^2 - 1 - 2(\zeta - 1)^{1/2}(\zeta - d^2)^{1/2}]\,d\zeta}{[\zeta(\zeta - 1)(\zeta - d^2)]^{1/2}}$$

$$= \frac{i}{(d + 1)(d^2 - 1)^{1/2}}\left\{2\zeta^{1/2}[(\zeta - 1)^{1/2} - (\zeta - d^2)^{1/2}]\right.$$

$$\left. - d\log\frac{[(\zeta - 1)^{1/2} - \zeta^{1/2}][(\zeta - d^2)^{1/2} + \zeta^{1/2}]}{[(\zeta - 1)^{1/2} + \zeta^{1/2}][(\zeta - d^2)^{1/2} - \zeta^{1/2}]}\right\}. \tag{20}$$

As $\zeta \to \infty$, $z \to ih$, so the following relationship between d and Λ is obtained from (20):

$$\Lambda = \left(\frac{d - 1}{d + 1}\right)^{1/2} + \frac{2d\log d}{(d + 1)(d^2 - 1)^{1/2}}. \tag{21}$$

Λ is real for $d \geq 1$ and confirms the previous expectation on d. Fig. 4 shows the dependence of Λ on d. For the range of Λ from 0 to 1 there is a one-to-one correspondence between Λ and d for the range $1 \leq d \leq 1.7101$. The horizontal width of the mid-section $|AA'|$ is given by $2|z|$ at $\zeta = 1$. Eq. (20) yields

$$\frac{\Lambda}{h}|AA'| = \frac{4}{(d + 1)(d^2 - 1)^{1/2}}[(d^2 - 1)^{1/2} + d\tan^{-1}(d^2 - 1)^{1/2}]. \tag{22}$$

At $d = 1.7101$, Λ equals unity and $|AA'|$ is finite with

$$|AA'|/h = 3.03. \tag{23}$$

From Eq. (16), $b^2 = d/2$; therefore $b \geq 1$ when $d \geq 2$ and the corresponding inclination β at the point of inflection is given by Eq. (18) at $\zeta = b^2 = d/2$:

$$\beta = \tan^{-1}\left(\frac{2d - 1}{d - 2}\right)^{1/2} + 2\tan^{-1}\left[\frac{d - 2}{d(2d - 1)}\right]^{1/2}. \tag{24}$$

$\beta = \pi/2$ at $d = 2$ and β is not real for $d < 2$ as expected. For the interval $1 \leq d < 2$, b lies between $1/2$ and 1 and the image in the hodograph plane is given in Fig. 2. The

maximum velocity at B is obtained from Eq. (19),

$$w_b = \frac{-i[(2d^2 - d)^{1/2} + (2 - d)^{1/2}]^2}{(2d^2 - 2)^{1/2}[(2d^2 - d)^{1/2} + d(2 - d)^{1/2}]}.$$

It lies on the downward imaginary w-axis so long as $2 \geq d \geq 1$.

4. Results and discussion. The complex potential χ, the complex conjugate velocity w and the z-plane have now been related to the ζ-plane. These relations contain only one real constant $d \geq 1$. Point D is located at $\zeta = d^2$ while point A is at $\zeta = 1$. It is convenient to express the results in terms of the parameter d. Fig. 4 shows the relationship between d and the parameter $\Lambda = h/R$, with $R = \Gamma/(4\pi U)$. For $0 \leq \Lambda \leq 1$, there is only one value of d, i.e., there is only one merged solution. In the limit of $\Lambda \to 0$, the free streamline approaches a circle of radius $2R$. For $\Lambda > 0$, the maximum vertical height y_d, of the free stream is greater than $2R$ (Fig. 5) while both the maximum semi-horizontal distance across the free streamline x_c and the semi-horizontal distance x_a at $y = 0$ are both less than $2R$, as shown in Fig. 6. The shapes of the free streamline for $d = 1.2$, $\Lambda = 0.60136$ and $d = 1.7101$, $\Lambda = 1$ are shown in Fig. 7.

As shown in Fig. 4 and also from Eq. (21), Λ increases to a maximum and then decreases to unity as d increases from unity to infinity. The maximum Λ_m is 1.365 at $d = 5.496$. For $1 < \Lambda < \Lambda_m$ there are three possible solutions, two merged solutions corresponding to two values of b and one solution consisting of two isolated vortices. From Fig. 6 it is clear that the solution with the larger value of d will have a narrower

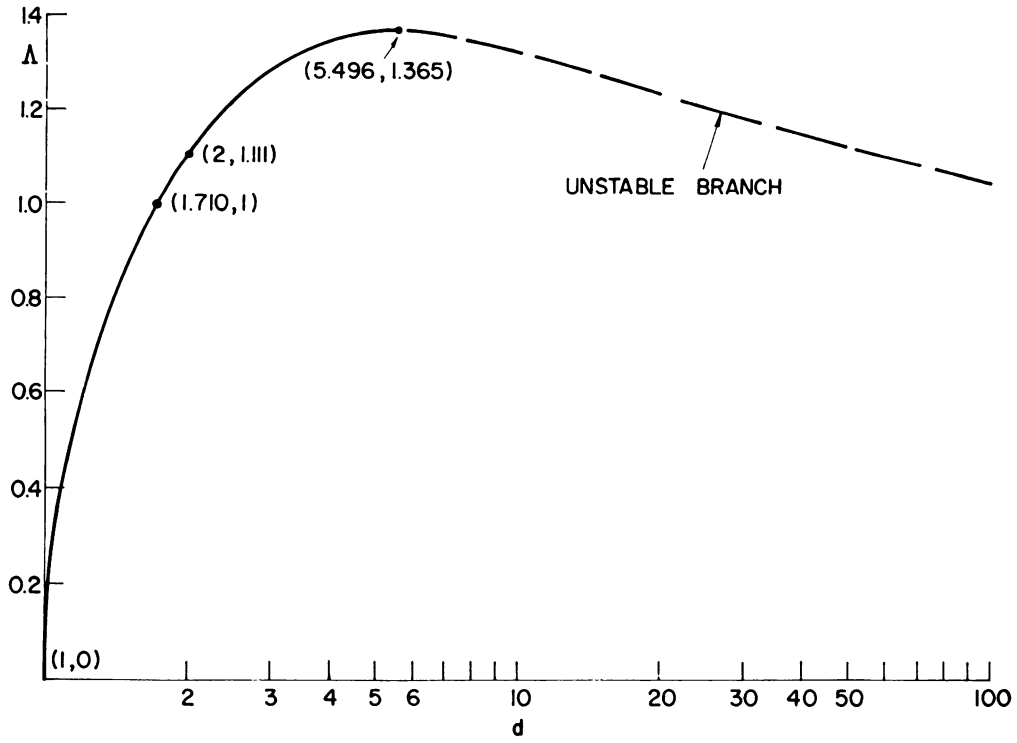

FIG. 4. The relationship between the parameter $\Lambda = h/R$ and the constant d in the ζ-plane.

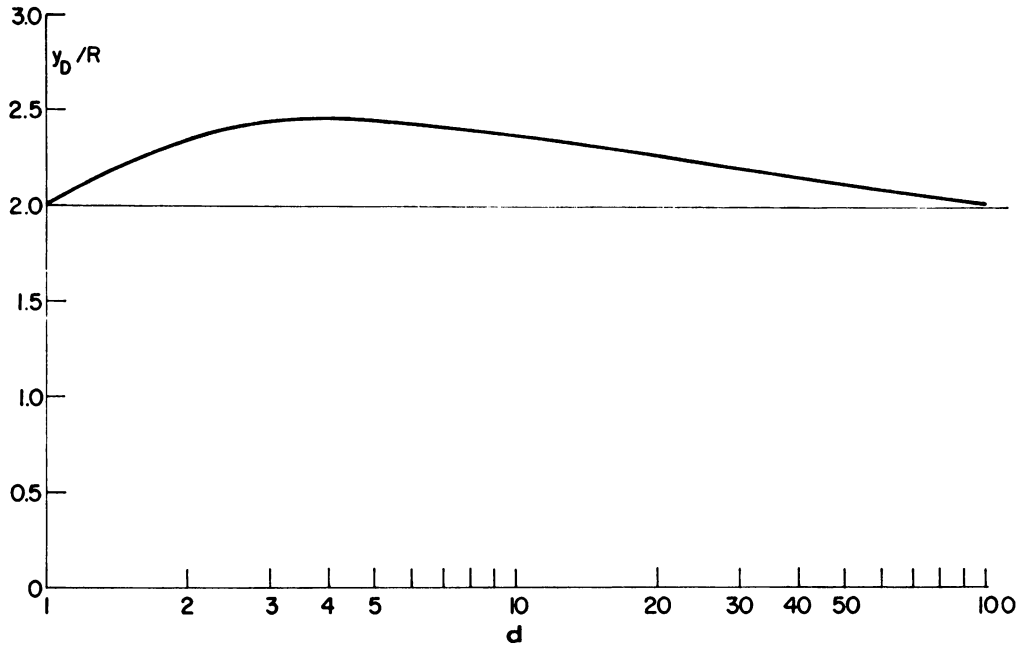

FIG. 5. Maximum semi-vertical height (y_d/R) of the free streamline.

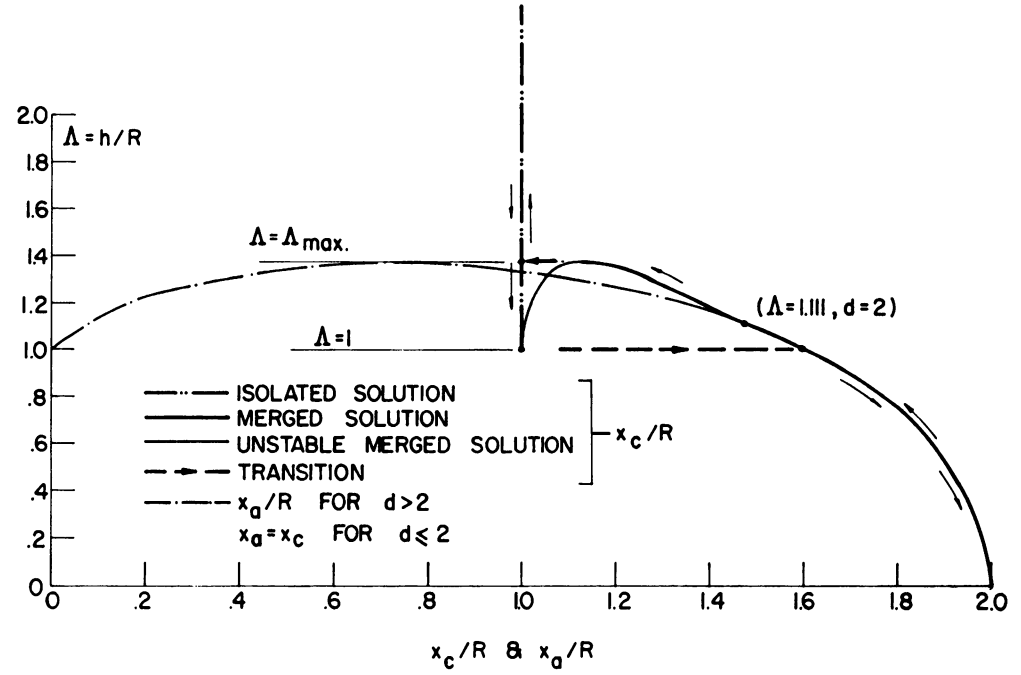

FIG. 6. Maximum semi-horizontal distance across the free streamline (x_c/R) and the distance at $y = 0$ (x_a/R).

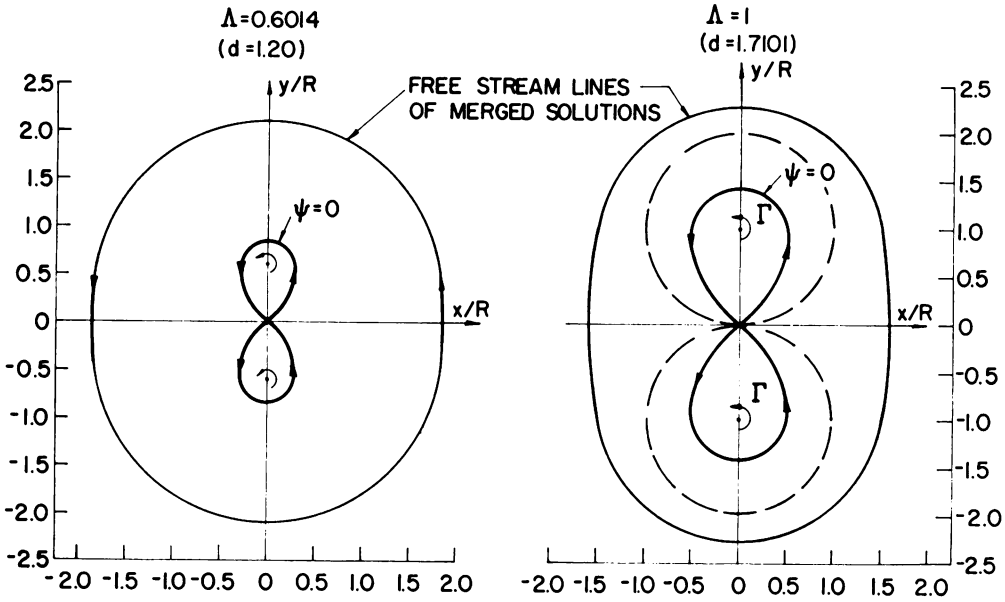

FIG. 7. The transition of the free streamline of the isolated solution (dotted line) to that of the merged solution as Λ decreases below 1. ($\psi = 0$ is the streamline of the merged solution passing through the stagnation point.)

neck (smaller x_a). From the analytical results of the preceding section and also from Fig. 6, the free streamline is convex for $d \leq 2$ with the maximum horizontal width at the middle ($y = 0$). For $d > 2$ the horizontal width at $y = 0$ becomes a local minimum and reduces to zero as $d \to \infty$. The shapes of the free streamlines for $d = 2$, $\Lambda = \Lambda_c = 1.111$, $d = 4$, $\Lambda = 1.347$ and $d = 5.496$, $\Lambda = \Lambda_m = 1.365$ are shown in Fig. 8. For the second and third cases, the free streamlines have local minimum sections at $y = 0$.

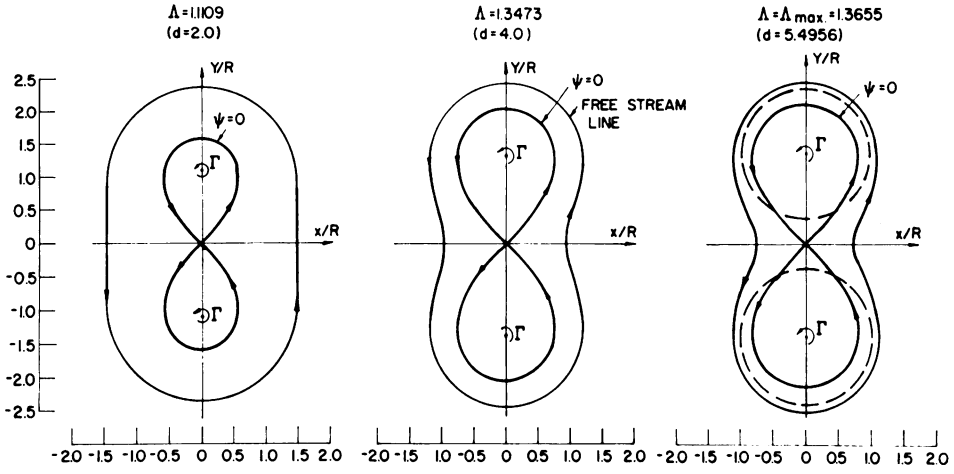

FIG. 8. The merged solutions as Λ increases and the transition of the free streamline to that of the isolated solution (dotted line). ($\psi = 0$ is the streamline of the merged solution passing through the stagnation point.)

It is clear that, for two vortices of given strength at a distance $2h$ apart with $h > R$ or $\Lambda > 1$, the solution is that of two isolated voritces. As h decreases to R, that is as Λ decreases to one, the solution changes suddenly from the isolated solutions inside two circles in contact to that of the merged solution with a convex free streamline (see Fig. 7). As h decreases further, $\Lambda < 1$, there is only one merged solution, as mentioned before.

If the flow field begins with a merged solution for $\Lambda < 1$, and then h increases gradually for fixed Γ, Λ increases and finally exceeds 1. It seems likely that the merged solution will continue along the d-Λ and the x_c-Λ curves in Figs. 4 and 6 from $\Lambda < 1$ to $\Lambda > 1$. For $\Lambda > \Lambda_c$, i.e. $d > 2$, the necking of the free streamline begins and finally at $\Lambda = \Lambda_{max}$, the merged solution inside a single free streamline breaks up into that of two isolated vortices (see Fig. 8). The right branch of the solution in Fig. 4 for $d > 5.496$ is probably unstable. These conjectures should be confirmed by additional theoretical analysis or by experiment.

References

[1] N. Levinson and R. M. Redhaffer, *Complex variables*, Holden-Day, 1970, pp. 289–297
[2] L. M. Milne-Thomson, *Theoretical hydrodynamics*, Macmillan, New York, 1955, pp. 301–333